AGU PUBLICATIONS

JGR

Journal of Geophysical Research: Oceans

RESEARCH ARTICLE

10.1002/2015JC011607

Atmospheric forcing during active convection in the Labrador Sea and its impact on mixed-layer depth

Lena M. Schulze[1], Robert S. Pickart[2], and G. W. K. Moore[3]

[1]Florida State University, Tallahassee, Florida, USA, [2]Department of Physical Oceanography, Woods Hole Oceanographic Institute, Woods Hole, Massachusetts, USA, [3]Department of Physics, University of Toronto, Toronto, Ontario, Canada

Key Points:
- Well-defined storm tracks toward Greenland result in the largest heat fluxes in the Labrador Sea
- The canonical low-pressure system that drives convection is located east of the southern tip of Greenland
- Deeper mixing in the western basin is due to higher heat fluxes rather than oceanic preconditioning

Correspondence to:
L. M. Schulze,
lschulze@fsu.edu

Citation:
Schulze, L. M., R. S. Pickart, and G. W. K. Moore (2016), Atmospheric forcing during active convection in the Labrador Sea and its impact on mixed-layer depth, *J. Geophys. Res. Oceans*, *121*, 6978–6992, doi:10.1002/2015JC011607.

Received 23 DEC 2015
Accepted 29 AUG 2016
Accepted article online 1 SEP 2016
Published online 22 SEP 2016

Abstract Hydrographic data from the Labrador Sea collected in February–March 1997, together with atmospheric reanalysis fields, are used to explore relationships between the air-sea fluxes and the observed mixed-layer depths. The strongest winds and highest heat fluxes occurred in February, due to the nature and tracks of the storms. While greater numbers of storms occurred earlier and later in the winter, the storms in February followed a more organized track extending from the Gulf Stream region to the Irminger Sea where they slowed and deepened. The canonical low-pressure system that drives convection is located east of the southern tip of Greenland, with strong westerly winds advecting cold air off the ice edge over the warm ocean. The deepest mixed layers were observed in the western interior basin, although the variability in mixed-layer depth was greater in the eastern interior basin. The overall trend in mixed-layer depth through the winter in both regions of the basin was consistent with that predicted by a 1-D mixed-layer model. We argue that the deeper mixed layers in the west were due to the enhanced heat fluxes on that side of the basin as opposed to oceanic preconditioning.

1. Introduction

The Labrador Sea is an important site of middepth convection through which Labrador Sea Water (LSW) is formed. The Deep Western Boundary Current transports this water southward, making it an important factor in the Atlantic Meridional Overturning Circulation and ocean ventilation. This provides a climate connection between the high-latitude atmosphere and the middepth ocean. The strength of the convection varies interannually and intra-annually depending on multiple factors, including atmospheric forcing and the oceanic preconditioning of the region in which the overturning takes place.

Open ocean convection occurs as a result of large surface buoyancy loss associated with intense winter surface cooling. In the Labrador Sea this is usually the case when wind advects cold, dry air off continental Canada. In combination with this, boundary currents encircle the Labrador basin associated with doming of isopycnals offshore, reducing the stratification and thereby setting up favorable conditions for deep convection to occur [*Marshall and Schott*, 1998]. However, in some years, strong near-surface stratification can reduce the depth of mixing. An example of this is the complete shutdown of deep water formation that occurred during the Great Salinity Anomaly in the early 1970s. During this time a large amount of freshwater was advected into the Labrador Sea [*Dickson et al*., 1988] which, combined with weak atmospheric forcing [*Gelderloos et al*., 2012], resulted in a 4 year period of no-deep convection. Modeling work suggests a strong relationship between the strength of subpolar salinity anomalies and the overturning circulation in the basin [*Gelderloos et al*., 2012], implying that such salinity anomalies also weaken the global overturning cell [*Broecker*, 1991].

Historically, it has been thought that the production of LSW is, to first order, dictated by the strength of the North Atlantic Oscillation (NAO) which is the leading mode of atmospheric variability over the North Atlantic [*Hurrell et al*., 2001]. A high NAO index reflects a strengthening of the westerly winds, with a greater number of low-pressure systems and a shift of storm tracks to a more northeasterly orientation [*Dickson et al*., 1996]. These conditions would favor convection in the Labrador Sea; more cold air from continental Canada would be drawn over the warmer surface waters of the Labrador Sea, subsequently causing increased air-sea buoyancy fluxes. However, the relationship between the NAO and convection is not simply linear, as there are other factors at play. For example, the strength of the air-sea fluxes in the Labrador Sea varies with the

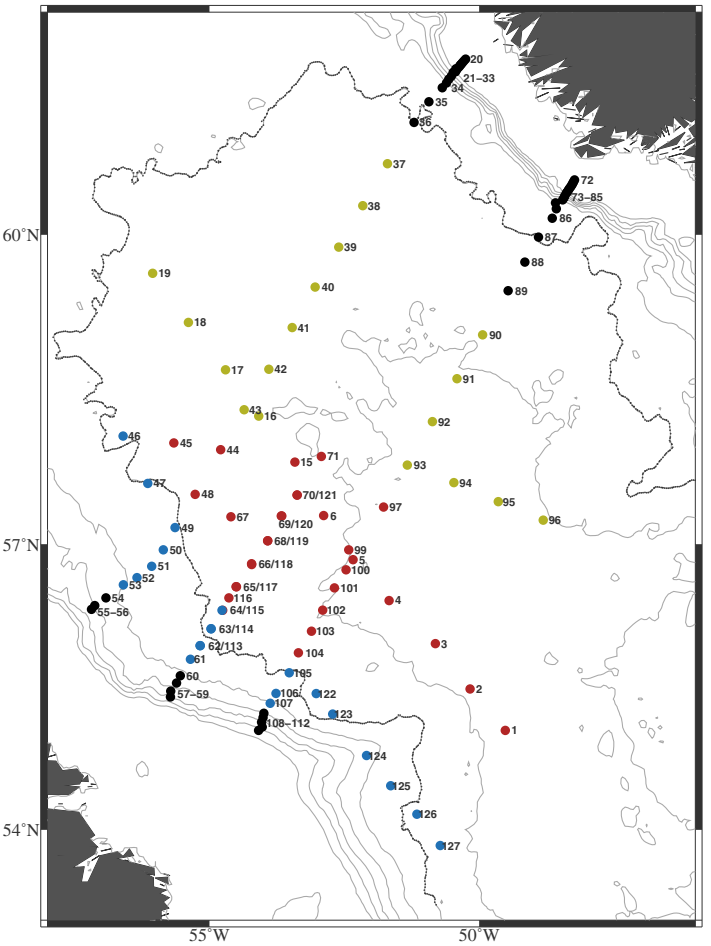

Figure 1. Locations of the CTD stations occupied during the February–March 1997 hydrographic survey. The colored circles show the stations in the boundary current region (blue), western basin (red), and eastern basin (yellow). The black stations are not included in the study since they are shallower than 500 m or have mixed layers less than 100 m. Note that the middle section in the west was occupied twice and some stations therefore have two station numbers. Gray contours show the isobaths with 500 m spacing, starting at 500 m. The black contour denotes the 3000 m isobath.

changing location of the northern center of the NAO, the Icelandic Low [*Serreze et al.*, 1997; *Moore et al.*, 2013], and depends as well on the detailed spatial distribution of the pack-ice [*Moore et al.*, 2014].

The relationship between the NAO index and Labrador Sea convection is further complicated by oceanic preconditioning, including the presence or absence of freshwater and eddies. A buoyancy cap can develop over the Labrador Sea basin after multiple years of weak overturning or as the result of large freshwater fluxes into the basin. This can make it harder for atmospheric forcing to remove this barrier and initiate convection, even under strong cooling and high NAO conditions. Conversely, successive winters of rigorous convection or a reduction of freshwater fluxes into the basin will result in a weakly stratified water column which is favorable for convection, even under mild forcing. This was the case during the winter of 1996–1997 when convection reached nearly 1500 m despite moderate surface forcing [*Pickart et al.*, 2002]. Eddies that form due to baroclinic instability of the boundary current system encircling the basin [e.g., *Spall*, 2004] are thought to be the most important mechanism through which freshwater and heat reaches the basin. The largest type of eddy, the Irminger Rings, can balance up to 80% of the seasonal heat loss to the atmosphere [*Katsman et al.*, 2004]. They are fundamentally important to the stratification of the Labrador Sea due to their warm and salty water at depth and cold and (seasonally) very fresh surface water [*de Jong et al.*, 2012].

Despite its importance, many aspects of LSW formation remain only partially understood, including the precise relationship between the hydrographic characteristics of the convected water column, the atmospheric forcing, and the preconditioning of the basin. This is partly because of the inherent difficulties in obtaining direct measurements of this process, and because the overturning is spatially and temporally variable. In some years, little to no-deep convection occurs, while in other years mixed layers can exceed 2000 m [*Rhines and Lazier*, 1995].

This paper investigates the relationship between the atmospheric forcing and the structure of the mixed layers during wintertime convection in the Labrador Sea. We use shipboard data from the Labrador Sea Deep Convection Experiment [*Marshall et al.*, 2002] that took place during the winter of 1996–1997. That winter was characterized by a moderate value of the NAO index, although the month of February 1997 had the second largest heat loss of all Februaries over the previous 20 years [*Pickart et al.*, 2002]. We begin with a description of the data and methods employed in the study. Next we investigate the atmospheric forcing

during the winter of 1996–1997, including the character of the storms and the resulting buoyancy fluxes. This is followed by a description of the bulk mixed-layer properties and their relationship to the forcing.

2. Data and Methods

2.1. Hydrographic Data

The primary oceanographic data used in this study were collected during a hydrographic cruise in the Labrador Sea from 2 February to 20 March 1997. The environmental conditions during the cruise, as described by *Pickart et al*. [2002], were favorable for overturning, with frequent storms resulting in strong winds and cold air temperatures. The mean wind speed during the 6 week period was 12 m/s out of the west-northwest with mean air temperatures of −8°C. During the cruise, multiple transects comprising a total of 127 conductivity-temperature-depth (CTD) stations were occupied (Figure 1; the middle section in the western part of the basin was occupied twice, separated by 10 days). A detailed description of the instrument performance, sensor calibration and accuracies, and data processing procedures are found in *Zimmermann et al*. [2000]. During the course of the cruise, three different CTDs were used. One of them was designated exclusively for towed sampling whose data are not included in this study. Here we use data from a NBIS Mark III CTD 9 and ICTD. A comparison cast of the two instruments showed very similar structure in the water column. Overall, the temperature and salinity accuracy was determined to be 0.001°C and 0.0025, respectively. For the present study we reprocessed the CTD data using the TEOS-10 equation of state. The downcast profiles used for the analysis consist of 2 db averaged bins.

2.2. Identification of Mixed Layers

For each profile the depth of the mixed layer was identified following the method described by *Pickart et al*. [2002, Figure 11]. Briefly, the mixed-layer depth was first estimated visually from the density profile, and the standard deviation in density was computed over this depth range. The depth at which the profile permanently passed out of the two-standard deviation envelope was then taken as the mixed-layer depth. In all but a few cases this technique returned unambiguous results. For the remaining profiles we applied the procedure to the individual traces of temperature and salinity, which cleared up any uncertainty. In this study only mixed layers exceeding 100 m from CTD stations occupied in water depths deeper than 500 m are considered (the colored stations in Figure 1). Of the 127 stations, 75 fulfilled these criteria. Notably, all of the mixed layers were stably (though weakly) stratified. As discussed in *Pickart et al*. [2002], some profiles showed multiple mixed layers, which meant that in total we considered 103 separate mixed layers. (Such stacked mixed layers are not the result of remnant mixed layers from the previous winter [see *Pickart et al*., 2002].)

2.3. Atmospheric Data

To characterize the atmospheric conditions during the winter of 1996–1997 we used the ERA-Interim reanalysis fields. These are produced by the European Center for Medium-Range Weather Forecasting and are described in detail by *Dee et al*. [2011]. The data were extracted for the period of 0600 UTC 1 December 1996 to 1800 UTC 31 March 1997 from the global analysis on a fixed grid with a 0.75° resolution and 6 h time interval. During the 1997 winter cruise, atmospheric measurements were taken. While this data set is too limited in space and time to be of use for the present study, the heat fluxes calculated using the shipboard measurements agreed well with those from the operational ECMWF analysis (which uses the same heat flux parameterization as the ERA-interim) following the ship track [*Renfrew et al*., 2002]. In general, however, during high wind events the errors in the ERA-interim values have been known to become significant due to the treatment of the ice-edge and surface heat flux algorithm in the presence of fractional ice cover that are not adequate for areas with large air-sea temperature differences [*Renfrew et al*., 2002; *Moore et al*., 2015]. In addition, there is evidence that the ERA-Interim product may underestimate surface wind speeds and air-sea heat fluxes over the Labrador Sea as a result of its horizontal resolution [*Moore*, 2014]. These limitations should be kept in mind when considering the results below.

2.4. Storm Tracking

Although automatic storm tracking methods have been used in previous studies [e.g., *Serreze et al*., 1997; *Zhang et al*., 2004], we chose to follow the method of *Pickart et al*. [2009] and perform this task manually using the ERA-Interim analysis fields. The domain for tracking the low-pressure systems extended from

120°W to 0°W and 20°N to 80°N. At each 6 h interval the coordinates and the central sea level pressure of the low were documented from its first appearance in the region to when the storm either exited the domain or dissipated. Oftentimes multiple storms were present in the study region which led to merging events, or a single storm would divide into two distinct systems. The main advantage of manually tracking storms is that such events do not escape detection and are less likely to be misrepresented.

This Lagrangian perspective regarding the trajectory of low-pressure systems is complemented using an Eulerian approach provided by the band-pass filtered standard deviation of the sea level pressure field [*Blackmon et al*., 1977]. In this framework, one typically uses a 2–6 day band-pass filter to isolate regions of high variability in the sea level pressure field associated with the motion of low-pressure systems, which is taken to denote the mean storm track [*Blackmon et al*., 1977].

2.5. One-Dimensional Mixing Model

To elucidate the ocean response to the atmospheric forcing during the convective season, a one-dimensional mixed-layer model [*Price et al*., 1986, hereafter PWP] was employed. To implement the model, fluxes of heat, freshwater, and momentum were imposed at the surface for each time step. We note that the results vary only slightly when wind stress is set to zero, and our main findings do not change when this is done. Mixing in the model is carried out until three different stability criteria are satisfied. These criteria are based on the vertical density gradient (static stability), the Richardson number (mixing layer stability), and the gradient Richardson number (shear flow stability) where the latter two reflect the wind mixing processes. The vertical grid of the model extends from the surface to 2500 m with 2 m resolution. At each time step (6 h), the model is forced with heat fluxes from ERA-Interim that are representative of the three Labrador Sea regions (Figure 1). When the above mixing criteria are satisfied, the depth of the mixed layer is identified as the first interface below the surface where the density jump exceeds a prescribed value.

3. Atmospheric Conditions

While oceanic preconditioning modulates the occurrence of convection in the Labrador Sea, the atmospheric forcing is a critical factor influencing the depth of convection in the basin [e.g., *Marshall et al*., 2002; *Sproson et al*., 2008; *Gelderloos et al*., 2012]. During winter the most prominent atmospheric feature in the North Atlantic is the Icelandic Low, centered southeast of Greenland [*Serreze et al*., 1997]. The cyclonic circulation associated with the Icelandic Low tends to advect cold air over the Labrador Sea [*Moore et al*., 2012] and results in a net transfer of heat from the ocean to the atmosphere. This is the primary driver of the convection that forms LSW. The long-term average turbulent heat flux in the basin during winter (November–February) is 270 W/m^2 [*Moore et al*., 2012] (in this paper positive heat fluxes refer to heat transferred from the ocean to the atmosphere). Typically, the heat flux increases by 17% in midwinter (January–February) compared to early winter (November–December), although the spatial pattern remains similar [*Moore et al*., 2012]. Here we describe aspects of the atmospheric circulation and heat fluxes in the Labrador Sea during winter 1996–1997 that had bearing on the development of the observed mixed layers.

3.1. Monthly Means

The month of December 1996 was anomalous in which the Icelandic Low was positioned to the south of its climatological mean position and was anomalously weak, with a trough extending northwestward into the Labrador Sea (Figure 2a). There was also a region of high pressure centered over the British Isles that may have been an atmospheric block [*Häkkinen et al*., 2011]. The sea level pressure (SLP) of the entire North Atlantic domain remained above 1006 mb and high pressure prevailed over the Nordic Seas. The average wind speed in the Labrador Sea was only 2.3 m/s, compared to the climatological average of 8 m/s [*Moore et al*., 2014]. The predominant wind direction was westerly, and heat fluxes barely exceeded 200 W/m^2 (Figure 3a). While January 1997 was colder and stormier, the conditions were also atypical compared to the long-term average [*Moore et al*., 2014]. There was still no signature of the Icelandic Low at its climatological location; instead, the Labrador Sea was characterized by relatively low SLP (as deep as 996 mbar). This was associated with northerly winds off the ice edge (Figure 2b) which led to enhanced heat fluxes over the western part of the basin (exceeding 300 W/m^2, Figure 3b). However, the winds remained anomalously weak, with an average speed of only 2.2 m/s.

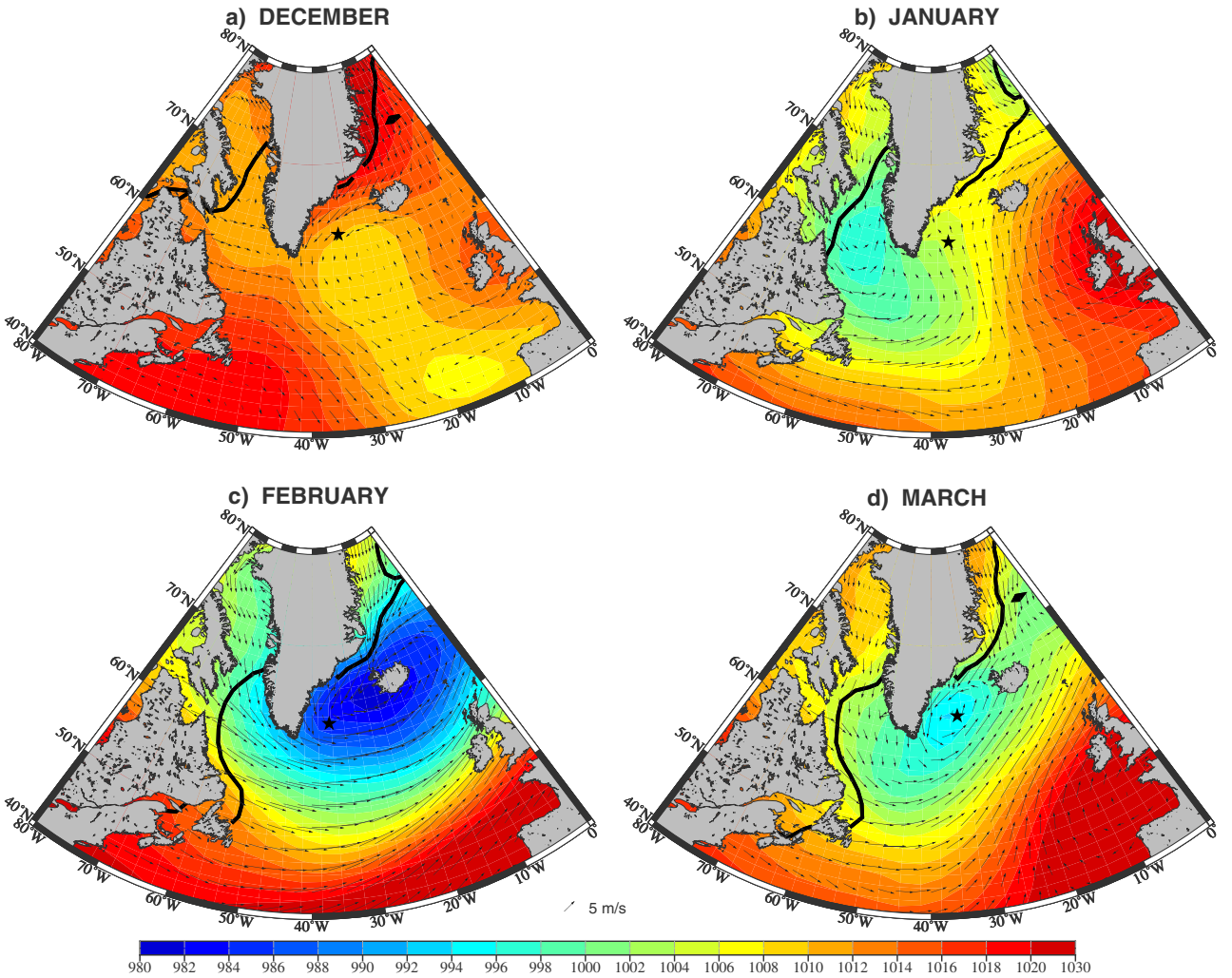

Figure 2. Monthly mean sea level pressure fields (color, mb), 10 m wind, (vectors, see key) and the 50% ice concentration contour (thick black contour) for (a) December 1996, (b) January 1997, (c) February 1997, and (d) March 1997. The climatological center of the Icelandic Low is indicated by the star, calculated from ERA-Interim for 1979–2015.

The situation changed drastically in February 1997. A deep Icelandic low developed (minimum SLP of 980 mb, Figure 2c) with strong northwesterly winds advecting cold air off the ice edge over the Labrador Sea (the average wind speed over the basin was 8.6 m/s). This resulted in strong turbulent heat fluxes that exceeded 500 W/m^2 along the western margin of the basin (Figure 3c). In March the Icelandic low was still close to its typical position but had filled considerably (minimum SLP of 992 mb, Figure 2d). Winds were still out of the northwest, but weaker than the preceding month (average wind speed of 3.5 m/s). As such, the average heat flux was lower, comparable to that in January (although the eastern part of the basin experienced stronger heat flux than in January, Figure 3d).

3.2. Storm Tracks

To shed light on the intraseasonal patterns described above, and in particular the reasons for the pronounced change in winds and heat flux over the Labrador Sea in February 1997, we analyzed the storm tracks over a broad region of the North Atlantic using the method described in section 2.5. In all, 85 storms were identified and tracked between December 1996 and March 1997 (Figure 4). Most storms were first detected over the North American continent or in the Gulf Stream region. However, some first appeared near the southeast tip of Greenland having spawned from a cyclone already in the area. This process is described by *Moore and Vachon* [2002], and results in the formation of secondary storms. In Figure 4 we have color-coded the trajectories by the central SLP of the storm. In general, there is a deepening of the low-pressure systems as they traverse from southwest to northeast along the North Atlantic storm track.

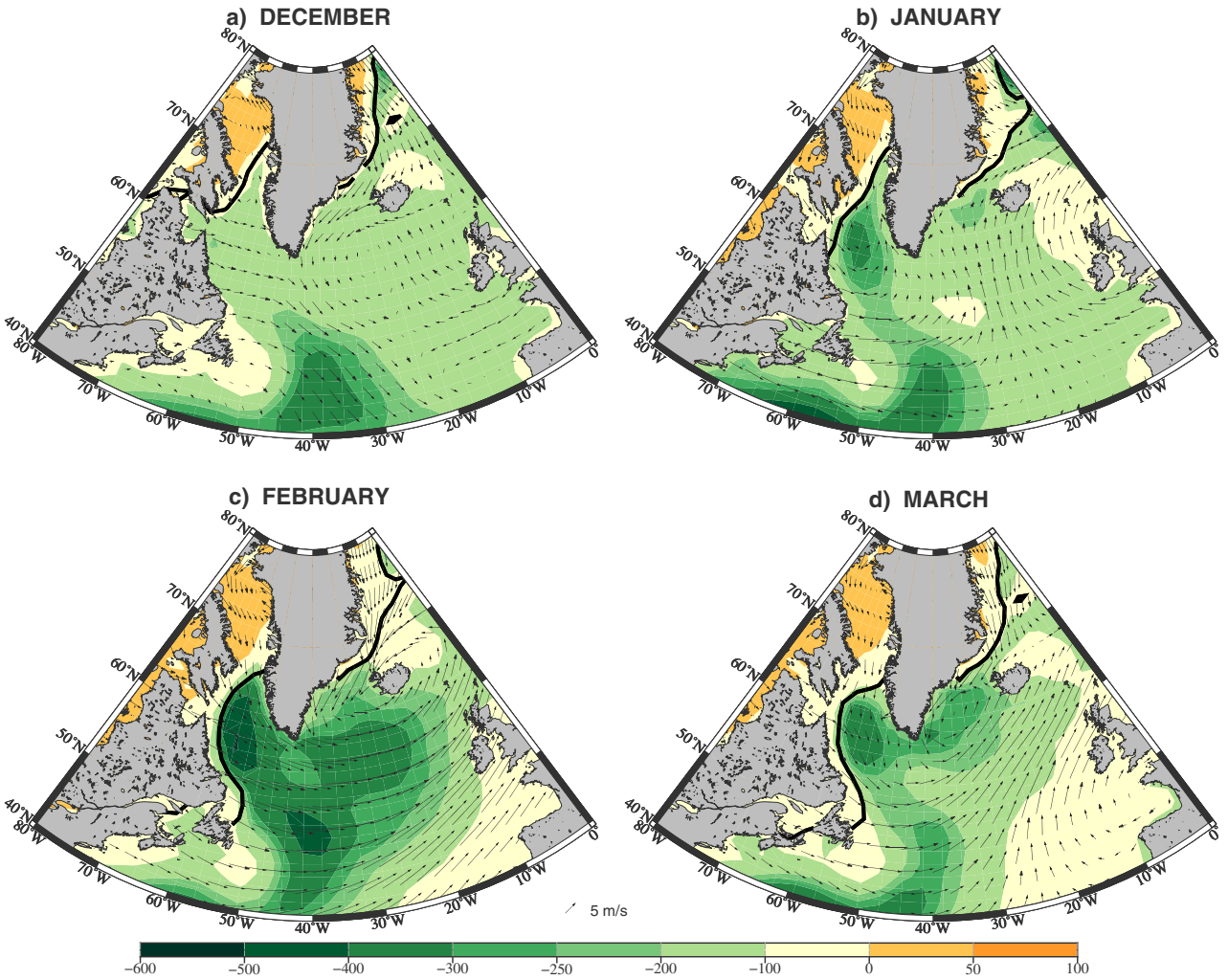

Figure 3. Same as Figure 2 except for total turbulent heat flux (color, W/m^2).

As noted above, December 1996 was an anomalously calm month. Remarkably, none of the cyclones crossed into the Irminger Sea where storms typically deepen, although some small storms still formed in this region (Figure 4a). Overall, the 26 storms in December were weak. Interestingly, there tended to be a bimodal pattern to their paths: a number of the storms traversed the North Atlantic from west to east, generally south of 60°N, while others veered northward and crossed the Labrador Sea. The former pattern resulted in the region of low SLP south of the Irminger Sea (Figure 2a). The latter pathway contributed to the weak winds and low heat fluxes in the Labrador Sea (since the winds are reduced in the vicinity of the storm center). Hence, it was not a lack of storm activity that led to the calm conditions in the Labrador Sea that month, but rather the position of the storm tracks.

Fewer storms (17) occurred during the month of January 1997 (Figure 4b). They were generally stronger in the subpolar part of the domain and had more organized tracks crossing the Atlantic from southwest to northeast. Some of the storms still veered northward, but only two crossed the Labrador Sea. Although only two storms entered the Irminger Sea, more of the low-pressure systems followed a path generally extending from Newfoundland toward the vicinity of Iceland. This in turn tended to draw some cold air from the Labrador landmass over the Labrador Sea (Figure 2b), and there were moderately strong heat fluxes over the western part of the basin (Figure 3b).

Although February 1997 experienced only three more storms than the previous month (20), there was a more clearly defined track oriented in the southwest-northeast direction. All of the systems following this track formed south of 50°N, many of them in the Gulf Stream region, and nine of them entered the Irminger

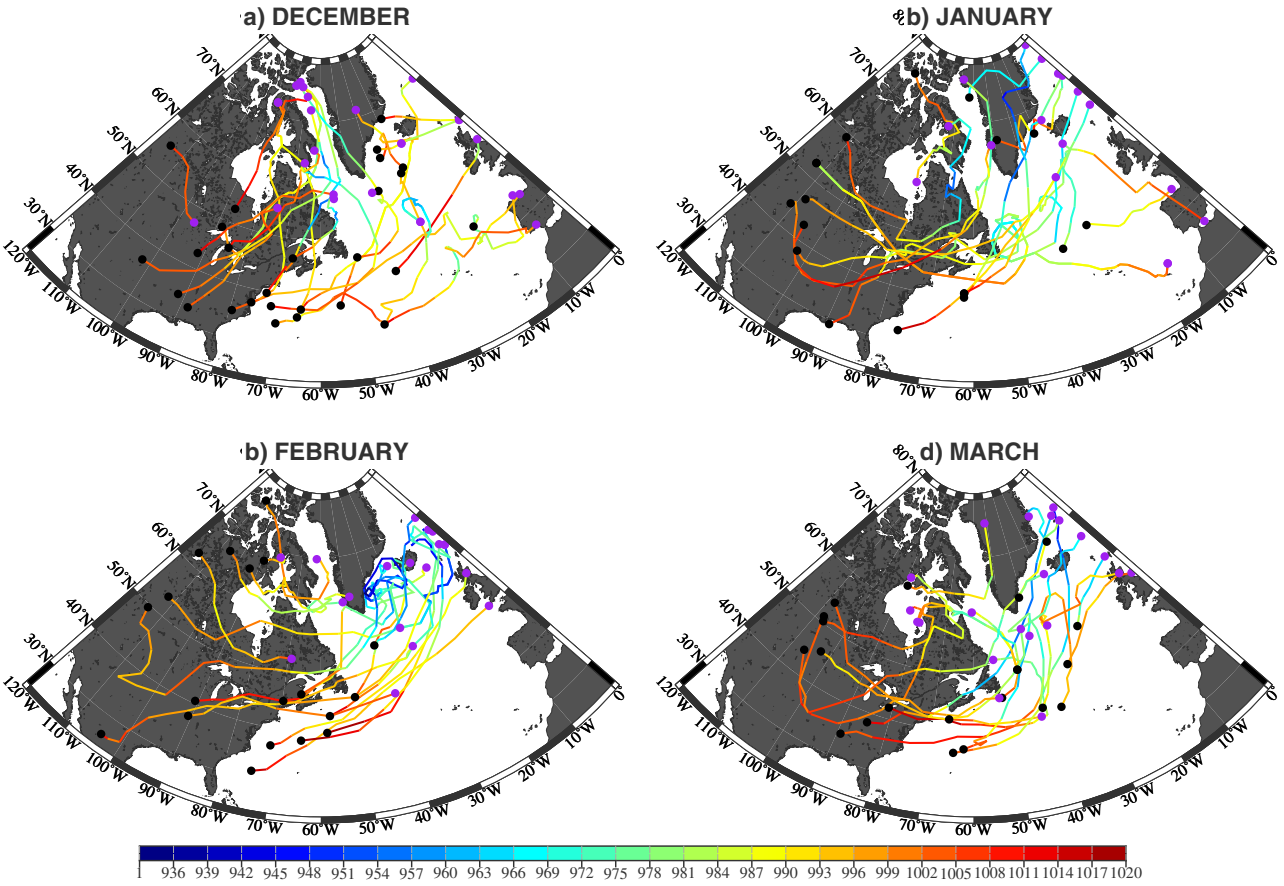

Figure 4. Cyclone tracks during (a) December 1996, (b) January 1997, (c) February 1997, and (d) March 1997. The tracks are colored by the corresponding sea level pressure observed at the center of the system at each position. Black circles denote the position at which the storm was first observed; purple circles show the last position of the storm in the domain.

Sea where they slowed and remained just off the east coast of Greenland. This is where they reached their minimum pressure (in the most extreme case, 940 mb). Of the seven storms that formed north of 50°N, only two (the two southern-most ones) reached the Irminger Sea. The others crossed the Labrador Sea from west to east before getting distorted by Greenland's topography. We note also that the storms that formed in the very southern part of the domain did not reach the Irminger Sea, but instead exited the region by passing south of Iceland. Hence, only the storms that formed in the latitudinal range 40°N–52°N (seven storms total) reached the typical position of the Icelandic low and deepened to pressures below 960 mb.

During March 1997 there were 22 storms, and, unlike February, only one of them formed in the northwest part of the domain (versus five the previous month). Furthermore, the storms that formed in the Gulf Stream region/eastern US tended to follow a similar southwest to northeast track as seen in February (although not quite as tightly confined). As such, one might have expected to see a similarly deep Icelandic Low in March as that which occurred in February. The reason this did not happen is that, while multiple storms crossed the Irminger Sea, only a single one remained in the region and deepened. The others storms traversed the region quickly, limiting their impact on the Labrador Sea.

We also computed the 2–6 day band-pass filtered standard deviation of the sea level pressure field during each month of the winter (Figure 5). This diagnostic is generally consistent with the patterns obtained from tracking the low-pressure systems. In particular, one sees that in December the region of largest variance extends northward from Newfoundland into the Labrador Sea due to the storms that veered northward into that area. The local maximum over the Irminger Sea during December is the result of the secondary lee cyclogenesis that occurred there, as noted above. In January there is evidence of an elongated region of elevated variance that extends from Newfoundland past Iceland into the Nordic Seas. This is consistent

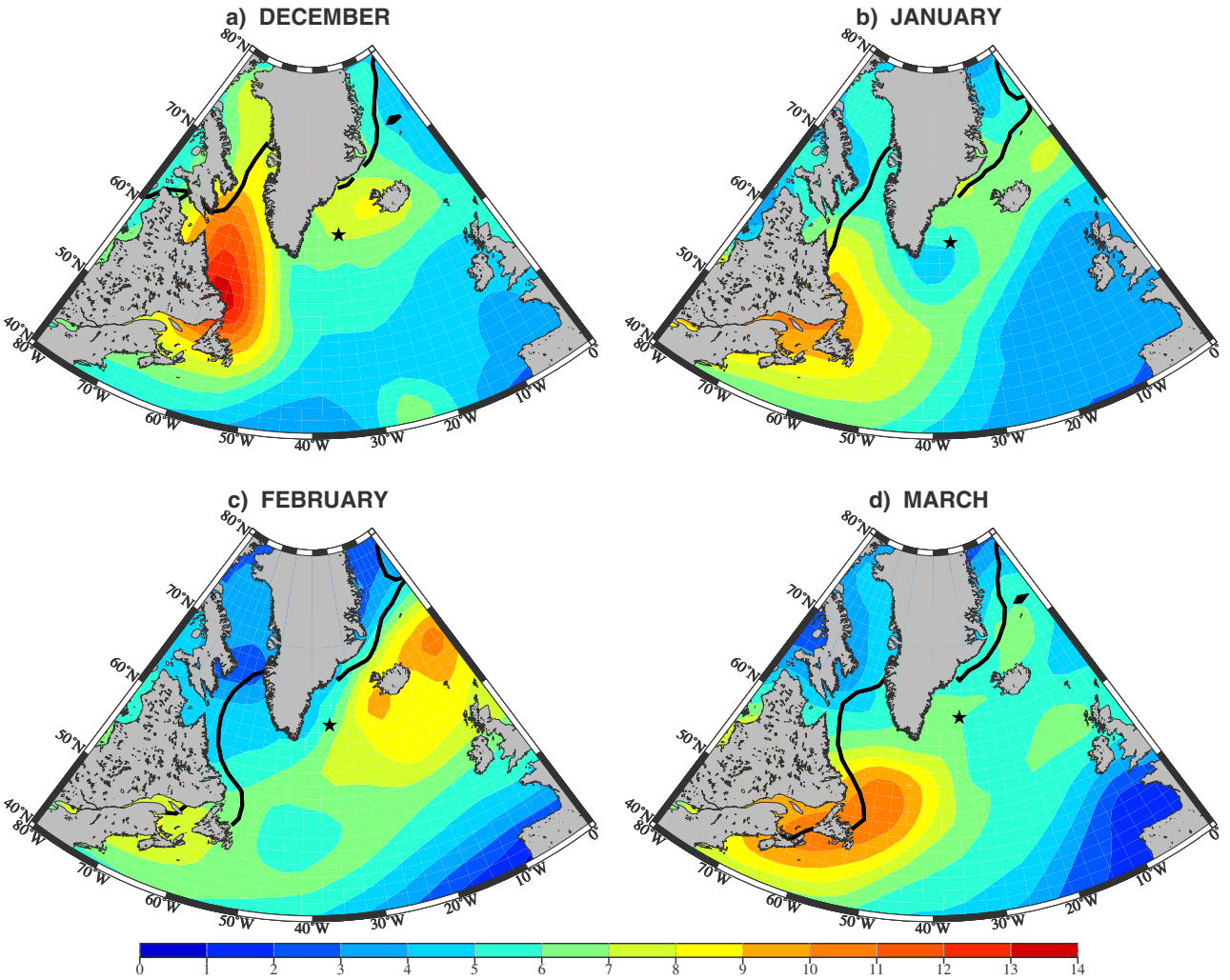

Figure 5. Same as Figure 2 except for 2–6 day band-pass filtered sea level pressure variance (color, mb).

with the more organized storm track that month, including the fact that most of the storms passed well to the southeast of Cape Farewell (hence, the minimum in variance immediately adjacent to southeast Greenland). While February also shows a well-defined region of elevated variance extending southwest to northeast, the degree of variability in the Irminger Sea is much greater than the previous month, reflecting the fact that the storms tended to deepen in this region during February. By contrast, the variance in the Irminger Sea decreases again in March because, as noted above, the storms traversed quickly through this region at the end of the winter.

To better understand what type of atmospheric conditions caused the largest heat fluxes in the Labrador Sea during winter 1996–1997, we employed the following methodology. The 6 h ERA-interim data were used to generate a time series of turbulent heat flux averaged over the interior Labrador Sea (black box in Figure 6). We define high heat flux events as times when the total turbulent heat flux in this region exceeded 400 W/m^2. This occurred during sixty-five 6 h time intervals (a total of approximately 16 days) over the course of the winter. All but two of the high heat flux events took place between mid-January and early March (Figure 6, top). In general, the winds were strong during this period (Figure 6, middle), but there was no statistically significant correlation between the heat flux and the wind speed. This reflects the importance of the air-sea temperature difference as well as the direction of the wind in dictating large cooling events.

To investigate this further, we constructed composite fields of the high heat flux events by averaging together all of the time periods during winter 1996–1997 when the mean heat flux within the box in Figure 6 exceeded 400 W/m^2. The purpose here was to reveal the canonical scenario resulting in the strongest air-

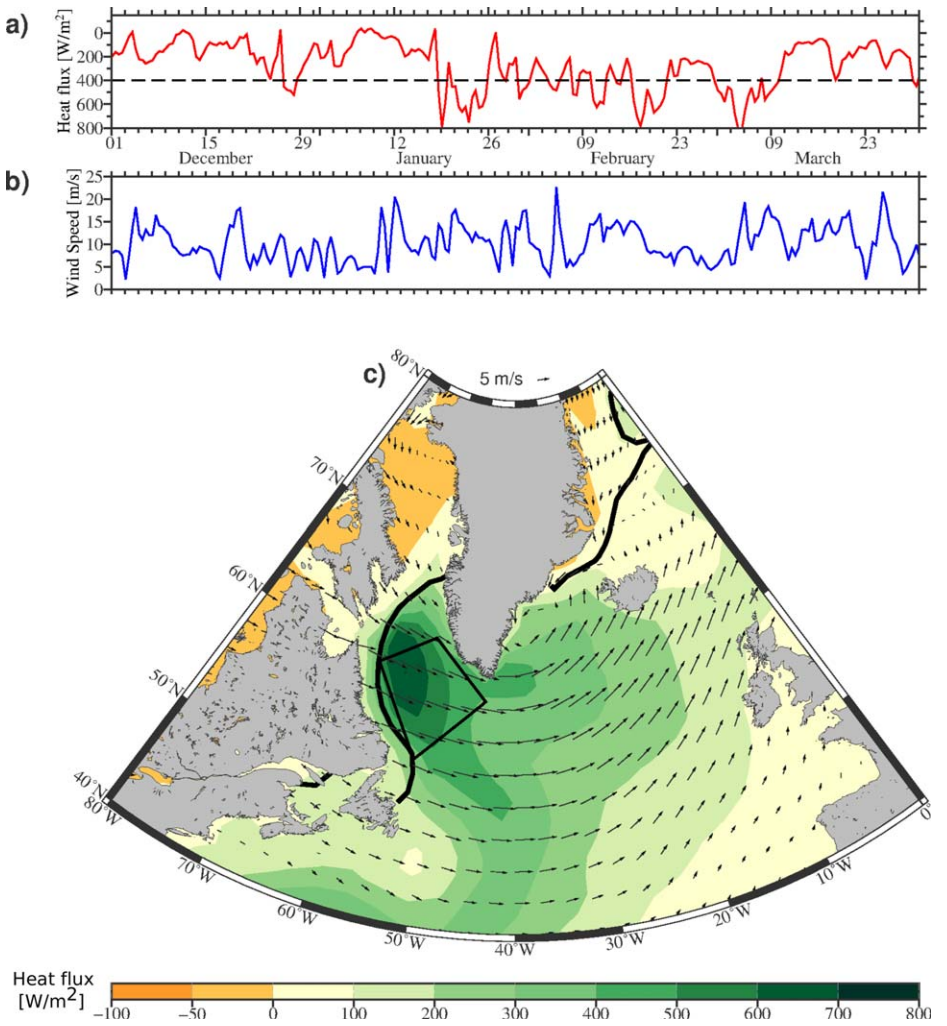

Figure 6. Time series of (a) total turbulent heat flux and (b) 10 m wind speed, averaged within the box in Figure 6c. In Figure 6a the 400 W/m^2 threshold is marked by the dashed line. (c) Mean turbulent heat flux field (color, W/m^2) for times when the heat flux in Figure 6a exceeded 400 W/m^2. The mean 10 m wind vectors are shown along with the 50% ice concentration isotac (thick black contour). The black box shows the region over which the turbulent heat flux and wind speeds were averaged in Figures 6a and 6b.

sea buoyancy fluxes in the Labrador Sea. As seen in Figure 7, this state is characterized by a region of low pressure situated offshore of the southeast Greenland coast with a central pressure of 984 mb. The wind speeds are elevated in a band around the southeastern/southern side of the low. Importantly, the wind direction in the Labrador Sea is nearly out of the west, i.e., directly off of the pack ice resulting in very cold air streaming over the warm ocean. Not surprisingly, the heat fluxes are strongest on the western side of the basin (Figure 6) with a maximum value $>$700 W/m^2 just seaward of the ice edge. It is also worth pointing out the region of enhanced heat flux to the east of Cape Farewell. This is the signature of westerly tip jets [*Moore and Renfrew*, 2005] which lead to convection in the Irminger Sea [*Pickart et al*., 2002]. In fact, the wind speed within the tip jets (up to 12 m/s) is higher than that in the Labrador Sea, indicating the importance of flow distortion by the high topography of Greenland (Figure 7).

We isolate the storms causing these high heat flux events in Figure 8, where the blue trajectories denote the storms in question and the red segments of the tracks indicate the times when the heat flux exceeded 400 W/m^2 in the Labrador Sea. The high heat flux storms occurred predominantly in January and February (five and seven storms, respectively), while in December and March only two storms each resulted in such large fluxes. There seem to be two scenarios that cause high heat loss in the Labrador Sea. The first is when storms progress into or near the southwest Irminger Sea (east of Cape Farewell), and the second is when they are in the vicinity of Baffin Bay (north of the Labrador Sea). All of the storms in February, except for

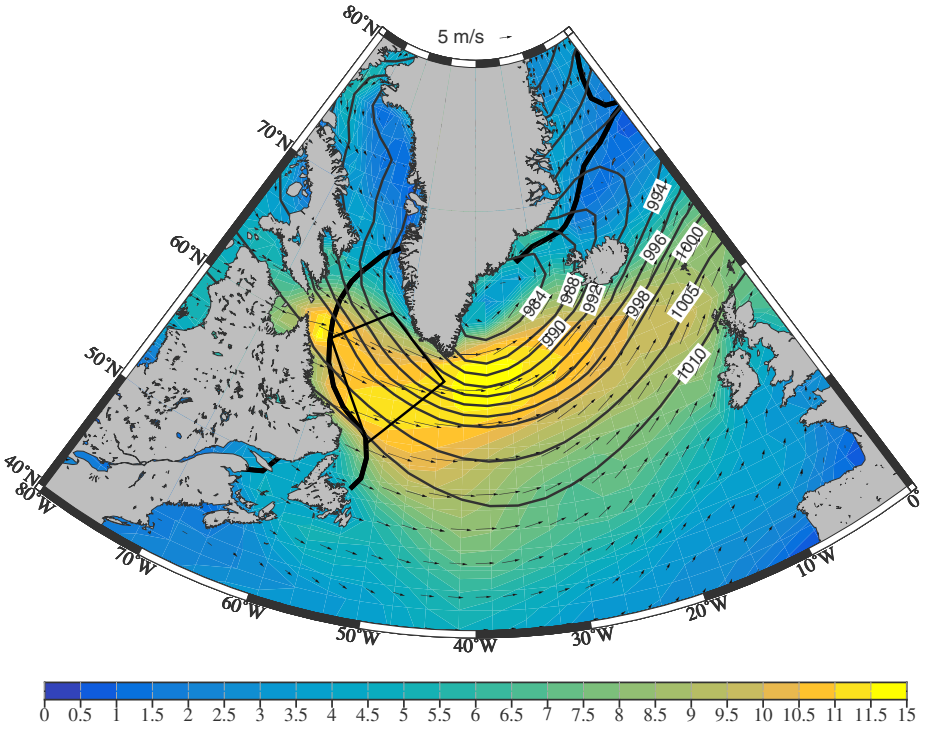

Figure 7. Same as Figure 6 except for the mean wind speed field (color, m/s) and the mean sea level pressure (contours, mb).

one, followed the former pattern. In particular, they slowed, reversed direction, and reached their deepest pressure over the Irminger Sea. The remaining storms (six storms in total) followed the latter course. Overall, the Irminger Sea route led to the most extreme heat loss events in the Labrador Sea.

4. Impact of Atmospheric Forcing on Mixed-Layer Depth

We now investigate aspects of the mixed layers that were observed during the February–March 1997 cruise and explore possible relationships to the atmospheric forcing.

4.1. Observed Mixed-Layer Depth

As detailed in Figure 1, we consider three different regions of the Labrador Sea: the western interior basin (red stations in Figure 1), the eastern interior basin (yellow stations), and the western boundary current (blue stations). The reason for this is as follows. In *Pickart et al.*'s [2002] study of the 1997 data set they noted a change in the T-S characteristics of the mixed layers between the western boundary current region and the interior. In particular, the remnant Irminger water resided roughly inshore of the 3000 m isobath where the mixed layers tended to be warmer and saltier. Furthermore, the ambient stratification is greater in this region and advective speeds are larger. Farther offshore, outside of the boundary current system, the ambient stratification is weaker and the circulation is more sluggish. We divided the interior basin into a western side and eastern side for two reasons. First, the atmospheric forcing varies across Labrador Sea; as noted above the heat flux is larger on the western half of the basin due largely to the proximity of the ice edge (Figure 3). Second, eddies containing Irminger water are often present on the eastern side of the basin [*Lilly et al.*, 2003] which impacts the stratification of the water column. We do not consider the stations on the shelf or in the vicinity of the shelf-break, or the stations on the west Greenland continental slope (because the atmospheric forcing is relatively weak there).

There are clear differences in the mixed-layer depths when distinguished geographically as such (Figure 9, top). For each region we plot the mixed-layer depth as a function of time. When a profile had more than one mixed layer, only the deepest is shown. Typically, several stations were occupied in a day, in which case each of the mixed-layer depths is plotted. Starting with the western basin, one sees that there is a clear

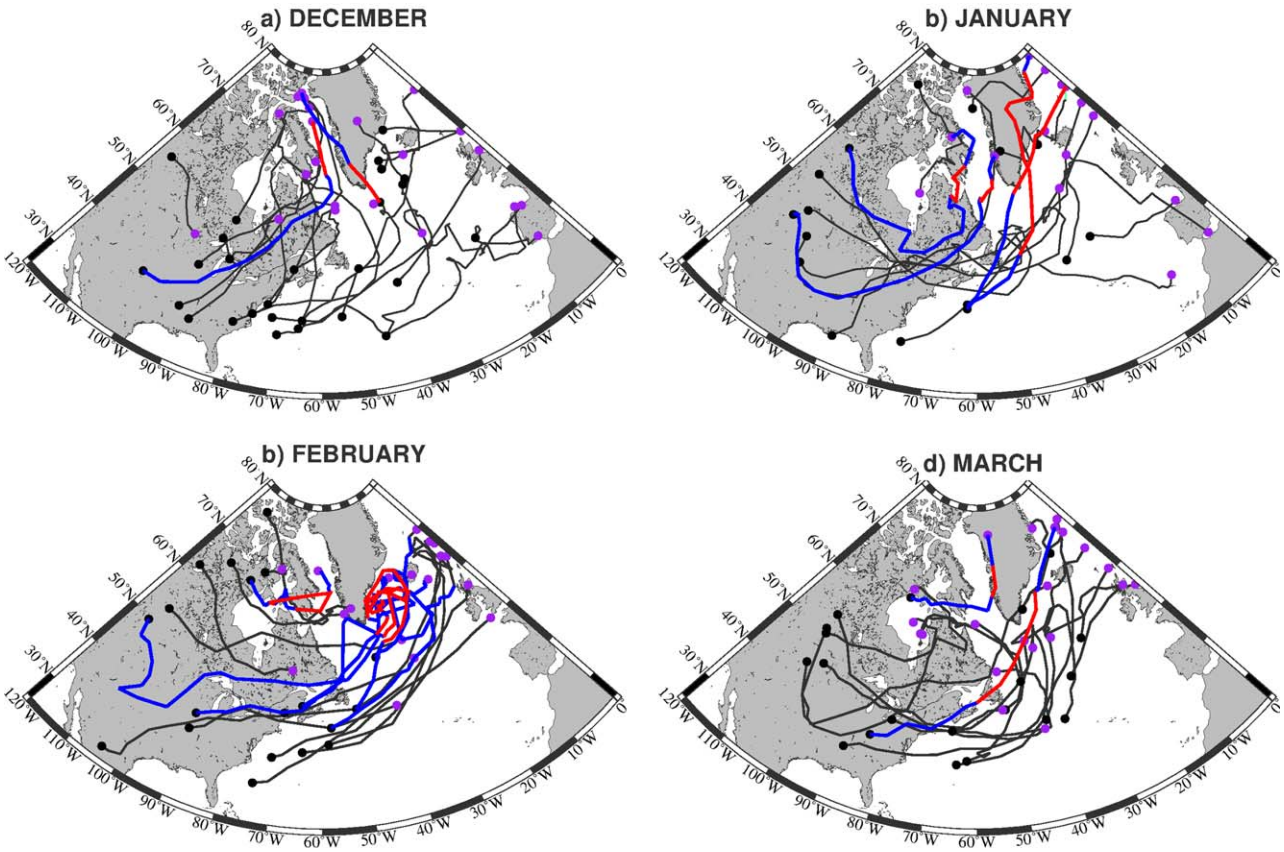

Figure 8. Storm tracks of the low-pressure systems that resulted in heat fluxes >400 W/m^2 within the box in Figure 6c. Storms during which this criterion was met are shown in blue with the red segments corresponding to the exact times when heat fluxes exceed 400 W/m^2.

trend toward deeper mixed layers as the winter progressed. It is in this region where the deepest mixing occurred, exceeding 1400 m in early March. Also in March, the observed daily scatter in mixed-layer depth increased.

While there were fewer stations occupied in the eastern basin, and no measurements past the beginning of March, it is nonetheless evident that short time/space-scale variability in mixed-layer depth was greater in this region than in the western basin. Some of the observed layers were on the order of 100–200 m, while others extended to 800–900 m. This variability can be explained in part by the Irminger eddies. As the ship approached the eastern side of the Labrador Sea, warmer, saltier, and shallower layers were occasionally observed that were indicative of convection into such an eddy (although this could not be verified because the features could not be resolved due to the relatively coarse station spacing).

The mixed layers in the boundary current region also displayed large variations between stations occupied close together in time and space. This might be explained to some degree by deformation of the convective plumes due to winds [*Straneo et al.*, 2002]. Furthermore, unlike the western interior basin, there is no indication of increased mixed-layer depths as the season progressed. This is perhaps not surprising because the convected water would be quickly advected to the south, replaced by water from upstream in the boundary current where the atmospheric forcing was not as strong. Nonetheless, despite the strong currents and greater stratification of the boundary current, deep mixing (to >1100 m) occurred in this region.

4.2. Predicted Mixed-Layer Depth

To assess the role of the surface buoyancy loss in dictating the observed variation in mixed-layer depth, we computed time series of total turbulent heat flux and wind stress representative of the western and eastern basins and used these to force the PWP model. The heat flux time series are shown in Figure 9 (bottom). For initial conditions we used hydrographic data collected on the WOCE AR7W section carried out in

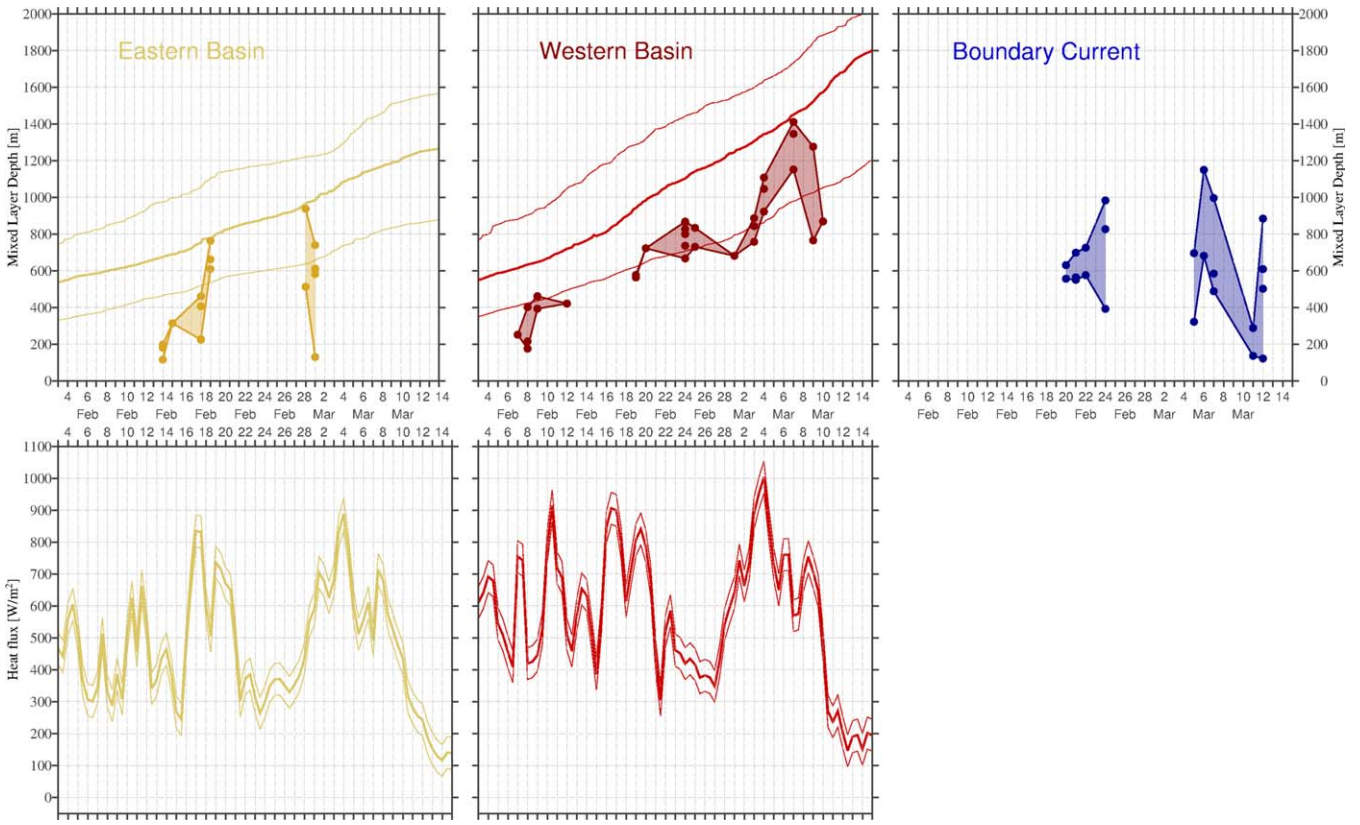

Figure 9. Top row: Mixed-layer depths for each region. Circles and shading show the observed mixed-layer depths from the CTD profiles. Stations taken farther apart than 7 days are not connected by a line. The thick solid lines show the predicted mixed-layer depth from the 1-D PWP model and the thin lines are the prediction using the mean forcing ± 50 W/m^2. Bottom row: Turbulent heat flux for each region; the mean heat flux is the thick solid line and the mean ± 50 W/m^2 are the thin lines.

October 1996. This section corresponds geographically to the southern transect occupied across the Labrador Sea during the winter cruise (stations 72–112, Figure 1). We averaged together the stations in the western and eastern basins, respectively, to create initial profiles (Figure 10, left) to be forced by the heat flux time series for the given region. The 1-D mixing model was run from October 1996 to mid-March 1997 (when the cruise ended) using these two regional heat flux time series.

The predicted mixed layers are shown in Figure 9 (top) for the time period of the cruise. Because of the uncertainty in the ERA-Interim heat fluxes, we carried out three different runs for each region: one for the computed heat flux (solid line in the figure), one where this value was increased by 50 W/m^2, and one where it was decreased by 50 W/m^2 (these are denoted by the dashed lines in the figure). According to *Renfrew et al*. [2002], the ERA fluxes in the Labrador Sea agreed to within 10–13% of the fluxes calculated using the shipboard data. Since the average fluxes in the interior portion of the Labrador basin are O(500 W/m^2), this dictated our choice of 50 W/m^2 for the uncertainty envelope. Considering the western basin first, during the time period of the cruise there were three pronounced storm events occurring in early February, mid-February, and early March. Each event was stronger than the preceding one. While it is evident that the model overpredicts the observed mixed-layer depths, the observations generally fall within the ± 50 W/m^2 envelope. When considering the locus of observed mixed layers (i.e., averaging out the scatter), it is seen that the mixed-layer depth increases more rapidly after the second storm event; this is true as well for the predicted mixed-layer depth.

While the number of sample days in the eastern basin is much less than that of the western basin, the comparison between the predicted and observed mixed-layer depths in the eastern region is nonetheless insightful. On this side of the Labrador Sea only the latter two storms (in mid-February and early March) stand out. As noted above, the short time/space-scale variability in observed mixed-layer depths in the eastern basin was quite pronounced due to the inhomogeneity of the water column, likely because of Irminger eddies. Considering again the locus of observations, there is a modest increase in mixed-layer depth over

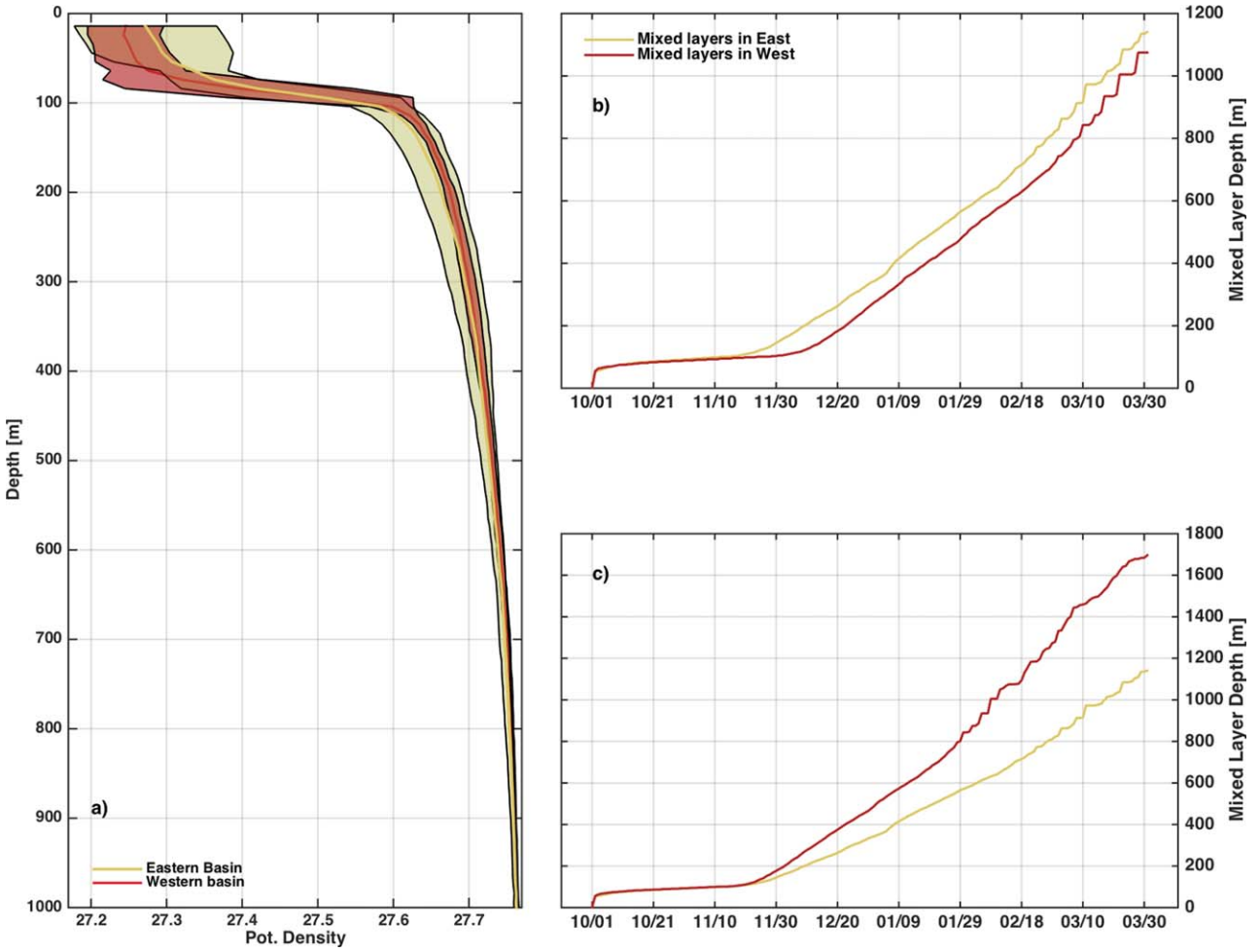

Figure 10. (a) Mean density profile and standard deviations (shading) of the eastern basin (yellow) and western basin (red) from the October 1996 AR7W CTD data. (b) Predicted mixed-layer depth for the eastern (yellow) and western (red) basin from the PWP model when forced with a constant heat flux of 500 W/m^2. (c) Same as Figure 10b except that the western profile has been forced with 600 W/m^2.

the 3 week period of measurements. This is consistent with the model prediction, and the deepest mixed layers observed during the two periods of sampling are in line with the PWP value (Figure 9).

While the increased scatter of the observed mixed layers in the eastern basin versus the western basin is seemingly due to the oceanic preconditioning (i.e., the presence of Irminger rings in the eastern basin), we argue that the deeper observed mixed layers in the west are the result of the stronger atmospheric forcing on that side of the Labrador Sea. This was assessed by running the PWP model with the same (constant) atmospheric forcing on both initial profiles (using 500 W/m^2, which is the average value over the interior Labrador Sea during the 6 week period of the cruise). In this case the mixed-layer depths on the eastern side were in fact deeper than those on the western side (Figure 10b). This is because the eastern initial profile has a weaker seasonal pycnocline (from approximately 80–100 m, Figure 10a), which erodes more quickly. Importantly, none of the stations on the eastern side of the 1996 AR7W line were occupied within Irminger eddies.

One might wonder if the weaker pycnocline in the eastern region was related to the extraordinarily strong convection in the Labrador Sea during the early to mid-1990s. To check this we scrutinized the available Argo float data from more recent winters (2002–2011) and found that, for non-eddy profiles, the eastern basin also had a weaker seasonal pycnocline. This implies that if it were not for the stronger atmospheric forcing in the west, the mixed layers in the eastern Labrador Sea would be just as deep as those in the western basin (outside of Irminger eddies). As a final calculation we ran the PWP model with stronger (constant) atmospheric forcing on the western initial profile (stronger by 100 W/m^2, which is the difference in the

mean values of the forcing in the western versus eastern basin (Figure 9, bottom row)). In this case the maximum predicted mixed-layer depth in the western basin was roughly 500 m deeper than for the eastern basin (Figure 10c), which is consistent with the observations.

While it is reasonable to apply a 1-D mixing model to the two interior basin regions due to the weak advection there, the boundary current was characterized by speeds as large as 40–50 cm/s. Hence, it should come as no surprise that the predicted mixed-layer depths displayed no relation to the observed depths in this region (not shown). This is in line with the absence of any trend over time in the observed mixed layers in this region (Figure 9).

5. Summary and Discussion

Using hydrographic data from a shipboard survey in February–March 1997 in the Labrador Sea, together with atmospheric data from a reanalysis product, we investigated the nature of the atmospheric forcing and its relationship to the observed mixed-layer depths. Even though the winter of 1996–1997 had a moderate NAO index, mixed layers exceeding 1400 m were observed due to preconditioning of the Labrador Sea during previous years. The early part of the winter (December and January) was uncharacteristically calm and warm with no sign of an Icelandic low in sea level pressure. Consequently, the heat fluxes were relatively low (100–300 W/m^2). In February the atmospheric conditions changed drastically. A deep Icelandic low developed and strong westerly winds drew cold, dry air over the warmer Labrador Sea, resulting in heat fluxes up to 600 W/m^2. In March the winds abated to some degree and the heat fluxes moderated, although the signature of the Icelandic low was still present.

A storm track analysis shed light on the conditions resulting in the highest heat fluxes during the winter of 1996–1997. Early in the winter, a significant number of the low-pressure systems progressing along the North Atlantic storm track veered into the Labrador Sea, which is generally not favorable for drawing cold air off of the Canadian continent. As the winter progressed, however, the storm tracks became more organized with a direct path into the Irminger Sea. Once in the vicinity east of Cape Farewell, the storms tended to slow down and sometimes backtrack—causing the Icelandic low sea level pressure signature that prevailed during the month of February. A composite average of the highest heat flux events in the Labrador Sea revealed that this scenario is most favorable for driving convection. Although the storms in March also generally progressed into the Irminger Sea, they traversed the sea quickly and, as such, did not have the chance to impact the Labrador Sea as effectively as during the previous month.

We divided the Labrador basin into three geographical regions: the eastern interior basin, western interior basin, and western boundary current region (shoreward of the 3000 m isobath). The time evolution and variability of the observed mixed layers were different in each of the regions. The deepest mixed layers were found in the western interior, while the station-to-station variability in mixed-layer depth was greater in the other two regions. In the eastern interior it was argued that this was due to the intermittent presence of Irminger rings, whose increased stratification would limit convection. The overall trend in mixed-layer depth through the winter in the two interior regions was consistent with that predicted by a 1-D mixed-layer model using data from the previous fall as the initial condition. By running additional cases with idealized forcing, it was demonstrated that the deeper mixed layers in the west were due to the enhanced heat fluxes on that side of the basin as opposed to oceanic preconditioning.

Similar conclusions regarding the influence of storm tracks on convection in the Labrador Sea were made by *Våge et al.* [2008]. They demonstrated that the deep convection observed in winter 2007–2008, which exceeded 2000 m, was partly due to storm tracks that followed a well-defined path from North America toward the Irminger Sea, similar to the storms observed here in February. Interestingly, the previous winter (2006–2007), which was characterized by a similarly high NAO index, did not result in significant convection due to a northward shift and less well defined storm tracks. Such a northward displacement of storm tracks is thought to be related to the Greenland Sea ice pack [*Dawson et al.*, 2002]. In light of the reduction of wintertime sea ice in the Greenland Sea over the past few decades [*Moore et al.*, 2015], this implies that, in the future, storms may tend to progress more readily into the Labrador Sea, with a concomitant reduction in heat fluxes. Notably, a northward shift of storm tracks in future climate conditions was observed in model simulations [*Bengtsson et al.*, 2005; *Ulbrich and Christoph*, 1999], and the response of the tracks to projected climate warming appears to be amplified in the Labrador Sea region [*Willison et al.*, 2013].

It is becoming clear that in order to predict the strength of convection in the Labrador Sea it is important not only to consider the NAO index but also the position of the Icelandic Low and the tracks of the individual storms. Our study, together with the results of *Våge et al.* [2008], indicate that the locations of the storms—and the speed that they travel—impact to first order the heat fluxes in the basin. The case study presented here for the winter of 1996–1997 motivates the need to consider other winters in comparable detail.

Acknowledgments
This work was funded by grant OCE-1259618 from the National Science Foundation (RP), the Natural Science and Engineering Research Council of Canada (GWKM), and the University of Southampton, Graduate School (LMS). The CTD data used in this study are available at http://rpickart.whoi.edu.

References

Bengtsson, L., K. Hodges, and E. Roeckner (2005), Storm tracks and climate change, *J. Clim.*, *19*, 3518–3543.
Blackmon, M. L., J. M. Wallace, N.-C. Lau, and S. L. Mullen (1977), An observational study of the northern hemisphere wintertime circulation, *J. Atmos. Sci.*, *34*, 1040–1053.
Broecker, W. S. (1991), The Great Ocean Conveyor, *Oceanography*, *4*(2), 79–89.
Dawson, A. (2002), Complex North Atlantic Oscillation (NAO) Index signal of historic North Atlantic storm-track changes, *Q. J. R. Meteorol. Soc.*, *12*, 363–369.
Dee, D. P., et al. (2011), The ERA-Interim reanalysis: Configuration and performance of data assimilation system, *Q. J. R. Meterol. Soc.*, *137*, 553–597.
de Jong, M., A. Bower, and H. Furey (2012), Two years of observations of warm-core anticyclones in the Labrador Sea and their seasonal cycle in heat and salt stratification, *J. Phys. Oceanogr.*, *44*, 427–444.
Dickson, R. R., J. Meincke, S. Malmberg, and A. J. Lee (1988), The Great Salinity Anomaly in the Northern North Atlantic 1968-1982, *Prog. Oceanogr.*, *20*, 103–151.
Dickson, R. R., J. Lazier, J. Meincke, P. Rhines, and J. Swift (1996), Long-term coordinated changes in the convective activity of the North Atlantic, *Prog. Oceanogr.*, *38*, 241–295.
Gelderloos, R., F. Straneo, and C. A. Katsman (2012), The mechanism behind the temporary shutdown of deep convection in the Labrador Sea: Lessons from the Great Salinity Anomaly year 1968-71, *J. Clim.*, *25*, 6743–6755.
Häkkinen, S., P. B. Rhines, and D. L. Worthen (2011), Atmospheric blocking and Atlantic multidecedal ocean variability, *Science*, *334*, 655–659.
Hurrell, J. W., Y. Kushnir, and M. Visbeck (2001), The North Atlantic Oscillation, *Science*, *291*, 603–605.
Katsman, C., M. Spall, and R. S. Pickart (2004), An estimate of eddy-induced circulation in the Labrador Sea, *J. Phys. Oceanogr.*, *34*, 1967–1983.
Lilly, J., P. B. Rhines, F. Schott, K. Lavender, J. Lazier, U. Send, and E. D'Asaro (2003), Observations of the Labrador Sea eddy field, *Prog. Oceanogr.*, *59*, 75–176.
Marshall, J., and F. Schott (1998), Open-ocean convection: Observations, theory and models, *Rev. Geophys.*, *37*, 1–64.
Marshall, J., et al. (2002), The Labrador Sea deep convection experiment, *Bull. Am. Meteorol. Soc.*, *79*, 2033–2058.
Moore, G. W. K. (2014), Mesoscale structure of Cape Farewell Tip Jets, *J. Clim.*, *27*, 8956–8965.
Moore, G. W. K., and I. A. Renfrew (2005), Tip jets and barrier winds: A QuickSCAT climatology of high wind speed events around Greenland, *J. Clim.*, *18*, 3713–3725.
Moore, G. W. K., and P. W. Vachon (2002), A polar low over the Labrador Sea: Interactions with topography and an upper-level potential vorticity anomaly, and an observation by RADARSAT-1 SAR, *Geophys. Res. Lett.*, *29*(16), 1773, doi:10.1029/2001GL014007.
Moore, G. W. K., I. A. Renfrew, and R. S. Pickart (2012), Spatial distribution of air-sea heat fluxes over the sub-polar North Atlantic Ocean, *Geophys. Res. Lett.*, *39*, L18806, doi:10.1029/2012GL053097.
Moore, G. W. K., I. A. Renfrew, and R. S. Pickart (2013), Multidecadal mobility of the North Atlantic Oscillation, *J. Clim.*, *26*, 2453–2466.
Moore, G. W. K., R. S. Pickart, I. A. Renfrew, and K. Vage (2014), What causes the location of the air-sea turbulent heat flux maximum over the Labrador Sea?, *Geophys. Res. Lett.*, *41*, 3628–3635, doi:10.1002/2014GL059940.
Moore, G. W. K., K. Vage, R. S. Pickart, and I. A. Renfrew (2015), Decreasing intensity of open-ocean convection in the Greenland and Iceland seas, *Nat. Clim. Change*, *5*, 877–882.
Pickart, R. S., D. J. Torres, and R. A. Clarke (2002), Hydrography of the Labrador Sea during Active Convection, *J. Phys. Oceanogr.*, *32*, 428–457.
Pickart, R. S., G. W. K. Moore, A. M. MacDonald, I. A. Renfrew, J. E. Walsh, and W. Kessler (2009), Seasonal evolution of Alutian low pressure system: Implications for the North Pacific Subpolar Circulation, *J. Phys. Oceanogr.*, *39*, 1317–1339.
Price, J. F., R. A. Weller, and R. Pinkel (1986), Diurnal cycling: Observations and models of the upper ocean response to diurnal heating, cooling and wind mixing, *J. Geophys. Res.*, *91*, 8411–8427.
Renfrew, I. A., G. W. K. Moore, P. S. Guest, and K. Bumke (2002), A comparison of surface layer and surface turbulent flux observations over the Labrador Sea with ECMWF analyses and NCEP reanalyses, *J. Phys. Oceanogr.*, *32*, 383–400.
Rhines, P. B., and J. R. N. Lazier (1995), A 13-year record of convection and climate change in the deep Labrador Sea, in *Abstract Report of NOAA Principal Investigator's Meeting*, pp. 50-55, NOAA, Miami, Fla.
Serreze, M. C., R. Carse, and R. Barry (1997), Icelandic low cyclone activity: Climatological features, linkage with the NAO, and relationships with recent changes in the Northern Hemisphere circulation, *J. Clim.*, *10*, 453–464.
Spall, M. (2004), Boundary currents and watermass transformation in marginal seas, *J. Phys. Oceanogr.*, *34*, 1197–1213.
Sproson, D. A. J., I. A. Renfrew, and K. J. Heywood (2008), Atmospheric conditions associated with oceanic convection in the south-east Labrador Sea, *Geophys. Res. Lett.*, *35*, L06601, doi:10.1029/2007GL032971.
Straneo, F., M. Kawase, and R. S. Pickart (2002), Effects of wind on convection in strongly and weakly baroclinic flows with application to the Labrador Sea, *J. Phys. Oceanogr.*, *32*, 2603–2618.
Ulbrich, U., and M. Christoph (1999), A shift of the NAO and increasing storm track activity over Europe due to anthropogenic greenhouse gas forcing, *Clim. Dyn.*, *15*, 511–559.
Våge, K., R. S. Pickart, V. Thierry, G. Reverdin, C. M. Lee, B. Petrie, T. A. Agnew, A. Wong, and M. H. Ribergaard (2008), Surprising return of deep convection to the subpolar North Atlantic Ocean in winter 2007–2008, *Nat. Geosci.*, *2*, 67–72.
Willison, J., W. A. Robinson, and G. M. Lackmann (2013), The importance of resolving mesoscale latent heating in the North Atlantic Storm Track, *J. Atmos. Sci.*, *70*, 2234–2250.
Zhang, X., J. E. Walsh, J. Zhang, U. S. Bhatt, and M. Ikeda (2004), Climatology and interannual variability of Arctic cyclone activity: 1948–2002, *J. Clim.*, *17*, 2300–2317.
Zimmermann, S., T. K. McKee, R. S. Pickart, and W. M. Smethie Jr. (2000), KNORR 147 leg V hydrographic data report: Labrador Sea Deep Convection Experiment, *Tech Rep. WHOI-2000-05*, 92 pp., Woods Hole Oceanogr. Inst., Woods Hole, Mass.